

SECTION IMAGING BY COMPUTER CALCULATION

G. Muehlechner*

Nuclear-Chicago Corporation, Des Plaines, Illinois

and R. A. Wetzel

University of Virginia, Charlottesville, Virginia

Radioisotope distributions are generally imaged by a method of collimation which results in a two-dimensional projection of a three-dimensional distribution. The information which is lost in the process of reducing the distribution to two dimensions is generally regained by taking views at right angles to each other and mentally correlating the information. Although far from ideal, this approach is the best ordinarily available to physicians; undoubtedly, valuable additional information could be gained from a more precise knowledge of the actual three-dimensional distribution.

The problem of accurate reconstruction is two-fold in nature: (A) the information about the radioisotope distribution must be gathered in such a way that three independent coordinates are available for every "point source" or the three coordinates must be deduced from the information by some secondary process; (B) this three-dimensional density function must be presented to the physician in a meaningful and easily comprehensible format, preferably an image.

Displaying a three-dimensional density function is by no means an easy task. It involves a perceptual task that the human observer is rather unaccustomed to, namely that of seeing an object and simultaneously seeing all parts within that object. One possible solution consists in viewing a number of section views at different points in time, thus using time as one of the coordinates. If the observer can arbitrarily shrink and expand the time scale over a wide range, he may then either view individual section views or, by shrinking the time scale, view the whole distribution as a summation of individual section views almost simultaneously.

With this possibility in mind, attention was directed toward obtaining a large number of section views at different levels by correlating information

from a number of views taken at right angles to the plane of the section views.

MATHEMATICAL MODEL

Consider a radioisotope distribution in an x-y-z-coordinate system and subdivide the volume into a $40 \times 40 \times 40$ matrix of equal sides (Fig. 1). Each volume element within this matrix can be assigned a density value which is proportional to the concentration of the radioisotope within the element. An ideal radioisotope imaging camera equipped with a parallel-hole collimator looking at this distribution in the x-direction, i.e. with the detecting plane of the camera lying in a plane parallel to the y-z plane, will perform an integration in the x-direction and record a distribution in the form of a 40×40 matrix, each element of which will contain the sum of the 40 density values of the corresponding elements in the x-direction.

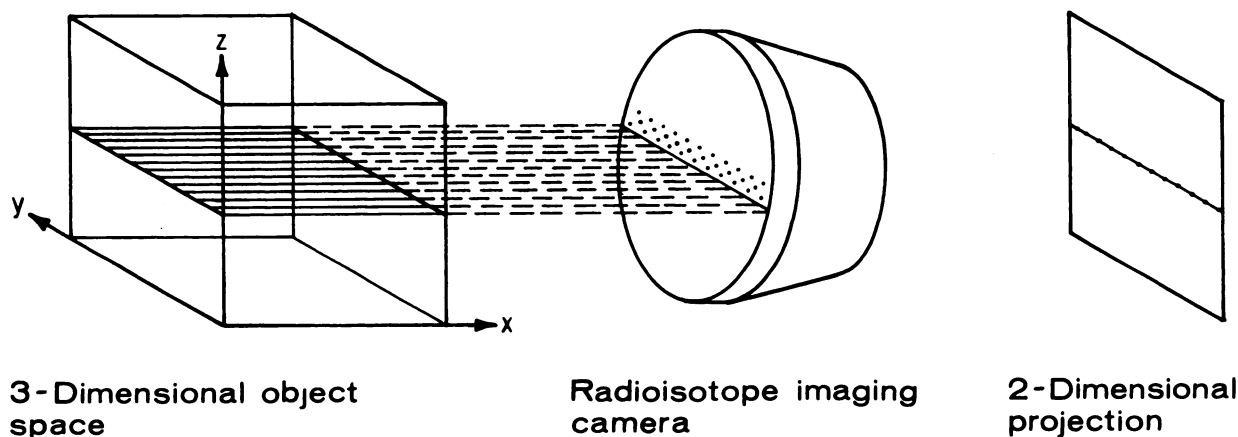
In this simplified model, the following factors have been ignored: (A) influence of statistical variations in the number of counts detected per element; (B) influence of absorption and scattering of the radiation in the object itself; (C) influence of the limited resolution of the camera and its variation as a function of depth.

The information about any plane parallel to the x-y plane is contained in the corresponding row of the two-dimensional projection. Since we wish to obtain a section view in the x-y plane, we need concern ourselves only with that plane and its corresponding row in the measured distribution. Clearly, more than one row of data is necessary to recon-

Received Jan. 6, 1970; revision accepted Oct. 5, 1970.

For reprints contact: Gerd Muehlechner, Deutsches Krebsforschungszentrum, Institut für Nuklearmedizin, 69 Heidelberg 1, Berliner Strasse 21, Germany.

* Present address: See above.



3-Dimensional object space

Radioisotope imaging camera

2-Dimensional projection

struct the original distribution; however, the total number should be kept to a minimum from a practical point of view. If the original distribution had to be calculated using a strict mathematical approach allowing only one solution, then a set of equations would have to be set up containing 1,600 unknowns and therefore requiring 1,600 data points. Recalculation of any arbitrary distribution in the plane of interest could then be performed. On the other hand, it could be argued that the location of a lesion such as a brain tumor is quite well known from only a lateral and an anterior or posterior view simply by looking at the two views. A closer examination of the problem shows that as more views are used in reconstructing the distribution the ambiguity in the location of the radioactive material is reduced. Since radioisotope distributions are smoothly-varying functions and since detail in any one plane is minimal—because of the actual distribution as well as the degradations introduced in the imaging process—a small number of views can be expected to allow a reasonably accurate reconstruction. A number of other factors influenced the final choice of eight views, spaced 45 deg apart in rotation around the center of the matrix, the most important of which are the following: (A) only symmetric arrangements were considered in order to avoid a significant dependence of the result upon the choice of the x- and y-axes in space, (B) calculations involving projections in the direction of the axes and along the diagonals are very simple compared to any other direction, and (C) a smaller number would introduce significant ambiguities in determining the distribution. As far as the mathematical model is concerned, opposing views are identical, reducing the number of views to four.

METHOD OF RECONSTRUCTION

Since an exact and unique solution is not possible with this limited amount of information, a method

FIG. 1. Radioisotope imaging process—showing projection of three-dimensional distribution onto two-dimensional plane and of plane onto line.

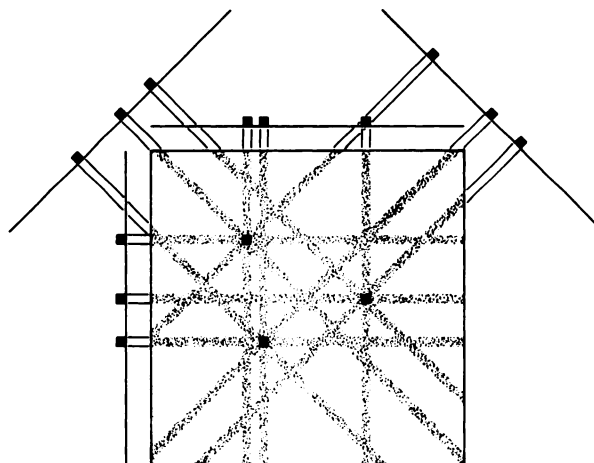


FIG. 2. Reconstruction of three point sources in plane from four rows of data.

of approximation must be found which maximizes detail but does not introduce significant artifacts. A rather crude form of reconstruction consists in superimposing the information from the four rows of data. Since each value in each row is the sum of all density values lying along a line perpendicular to the particular row, each value is divided by the number of matrix elements which could have contributed to the sum, and this value is assigned to every matrix element lying along that line (Fig. 2). The values thus assigned from every row are added. If three point sources are imaged using this procedure, the resultant image consists of three star-like patterns as shown in Fig. 2.

This procedure distributes density values over a larger area than necessary. A quick inspection of data rows permits determination of the maximum extent of the original distribution within an octagonal-shaped area. By distributing the density values only within this area, an improved image is obtained.

This process reduces the number of unknowns from 1,600; in a realistic situation a reduction by a factor of two is not uncommon.

The image thus obtained serves as a basis for reconstructing the original distribution. Every density in the original distribution contributes a star-like pattern to this image which is thus the sum of many of these patterns, each with a different amplitude. A number of methods can be devised to subtract the star-like pattern while retaining the intersection as the origin of the pattern from the original distribution. The following procedure proved to be most successful: the matrix of 1,600 elements is scanned, and all elements within a given percentage of the maximum density value are identified as centers of a star pattern—instead of being merely the sums of the “rays” from different star patterns (i.e., black squares in Fig. 2 compared with intersections of up to three “rays”). For each of the elements identified in this way the following operation is performed: (A) a constant is added to a second 1,600-element matrix at the coordinates of the identified element; (B) from each of the four rows of input data such an amount is subtracted that upon reconstruction by superposition the density value of that element and its corresponding star pattern is reduced. Upon reconstruction of the matrix from the four rows of

data by superposition the previously identified elements are now reduced in density, their corresponding star patterns are also reduced, and the new improved image consisting of the identified elements minus any star pattern is being constructed in the second matrix. The operation is repeated until the density values of all elements are reduced to a negligibly low level, thereby building up the reconstructed image in the second matrix. It should be mentioned at this point that many “reasonable” iteration schemes can and have been devised which either result in artifacts or in poor reconstructions. The described method proved to be most successful; several others were tried, and there may be a better one. Attempts to optimize the iteration procedure by a theoretical investigation were quickly abandoned because of the complexity of the problem.

Superposition of data from different directions as described above and as shown in Fig. 2 has been used previously to obtain section views (1-3) using either analog optical or digital methods. However, many views from many different directions were usually used in order to reduce the starlike artifacts apparent in Fig. 2. The iterative reconstruction method makes use of the fact that the point-source response function—namely the star pattern—is known; thus it uses a priori knowledge to improve upon the first reconstruction obtained by superposition. The use of the point-source response function to improve images of radioisotope distributions is not new, and many different processes have been used; these include iterative methods (4), filter methods (5), and dot shifting techniques (6). In most of these techniques the original picture can be processed to varying degrees with the result that the image begins to show unacceptable artifacts if either too many iterative steps are taken or if the filter is allowed to amplify high frequencies beyond a certain limit. The same applies to the iterative method described here. At this time we do not have a test which clearly predetermines the amount of processing permissible without producing artifacts of a given unacceptable level.

In order to clarify the iteration procedure used, a numerical example is given in Fig. 3. Instead of a 40×40 matrix, a 4×4 matrix was chosen to reduce the complexity, yet show the essential features of the process.

STEP 1 shows the distribution to be reconstructed, namely two “sources” with equal strength. The sources were assigned a density of 24 in order to keep the numerical example simple. The four rows of data, which are obtained by performing a summation along the columns, rows and diagonals of the matrix are also shown. They serve as the input

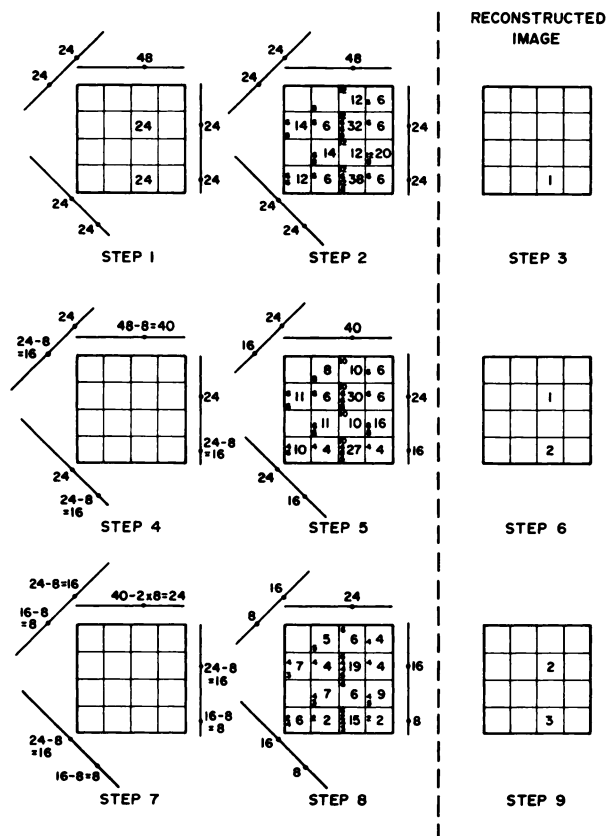


FIG. 3. Numerical example of iterative reconstruction process.

data to the reconstruction process. In STEP 2 the input values are divided by the number of matrix elements in the corresponding row, column or diagonal, and this value is entered on the left hand side of each matrix element. The sum of all values in each element is shown on the right side; these numbers represent a first approximation to the original distribution shown in STEP 1. All elements within five units (an arbitrary choice in this example, an input parameter affecting contract in the computer program) of the maximum summed value (38) are identified as centers of a star pattern; in this case only one such element exists. A constant, namely 1, is added to a second matrix at the coordinates of the identified element (STEP 3). For each of the four rows of input data a constant amount is subtracted from the number which contributed to the identified element (STEP 4). This has the effect that upon reconstruction as performed in STEP 2, the identified element as well as its corresponding star pattern is reduced in density (STEP 5). Again all elements within five units of the maximum are identified as centers of a star pattern; this time two elements are thus identified. The identified elements are increased by one in the second matrix (STEP 6) and a constant amount is subtracted from the input data corresponding to the identified elements (STEP 7). Note that both identified elements are in the same column and therefore the constant amount must be subtracted twice as shown. Upon reconstruction (STEP 8) again both elements are identified as centers of a star pattern. It is easy to see that carrying the process through STEPS 10, 11, 12 will complete the iteration, leaving two sources of equal strength in the proper elements in the second matrix.

In such a simple example artifacts are not present, in a complicated example, such as the one shown in Fig. 4A, artifacts as seen in Fig. 4B indeed are unavoidable since an accurate reconstruction is mathematically impossible.

This example demonstrates the iteration procedure only; in the actual computer program, the extent of the object is determined first and the number of unknowns is reduced by restricting the size of the matrix used in the reconstruction process.

MATHEMATICAL PHANTOM STUDY

The method described above of reconstructing the original distribution was tested on a number of mathematical phantoms, one of which will be described. The calculations were performed using an IBM 360/30 computer.

Density values from 0 to 10 are assigned to all matrix elements in a 40×40 matrix. These values are added up along both axes and the diagonals to

give four rows of numbers which are then used as the input data to the computer program. The reconstructed distribution is available as a number matrix as well as a CRT display in which the brightness is made proportional to the density value.

The phantom was prepared in the following way: an arbitrary shape was drawn onto a 40×40 matrix, and all matrix elements within this area were assigned a density value of two; all elements outside this area were assigned a value of zero. Into this area, four small rectangles of different sizes were drawn, and all elements inside this area were assigned a value of ten, resulting in a target-to-nontarget ratio of five (Fig. 4A). The sums were formed in the

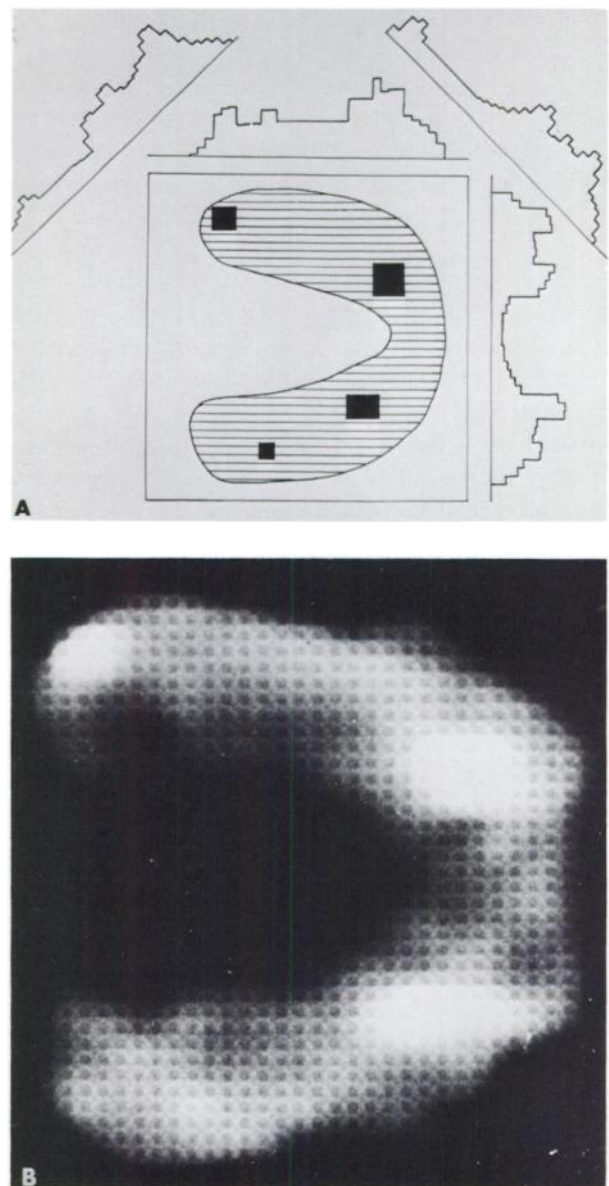


FIG. 4. A shows mathematical phantom and its four projections as histograms. B shows reconstructed phantom using projections as input data; brightness is proportional to calculated density.

fashion mentioned above to give four rows of input data which are drawn in the form of histograms in Fig. 4A. It should be noted that the distribution described is more complex than that likely to be encountered clinically for any given plane; also the variation in density values is certainly not excessive. By merely looking at the four histograms which serve as the only input to the computer program, very little can be deduced regarding the original distribution.

The reconstructed 40×40 matrix is shown in Fig. 4B, in which the brightness is proportional to the calculated density value. The shape is well reconstructed; three of the rectangles are clearly visible, while the smallest rectangle is barely visible. Numerous small computer-generated artifacts are visible as well. However, comparing the reproduction to the histograms makes it apparent that at the very least the process helps in visualizing the shape of an object and the location of structures and that possibly the process helps in detecting structures.

EXPERIMENTAL CONSIDERATIONS

After these encouraging results with a mathematical model, it was considered appropriate to investigate experimental problems by undertaking a phantom study and clinical evaluation. It was decided to focus attention first on brain studies for a number of reasons. The head can be imaged easily from all directions with the Anger scintillation camera intended to be used in this study. All of the activity is imaged completely from all sides without any activity appearing in one view and not another. This presents a serious but hopefully not insurmountable problem in the case of the liver where the spleen would interfere in some of the views. The brain is centrally located with nearly equal amounts

of absorbing tissue surrounding it on all sides, thus minimizing the problem of nonuniform tissue attenuation.

The problem of tissue attenuation is solved by taking opposing views and adding them. Column A in Table 1 shows the probability that a given gamma ray at 140 keV is absorbed or scattered in tissue-equivalent material as a function of distance from the surface for a total thickness of 14 cm which corresponds to the mean ear-to-ear width of the human head. Column B in Table 1 shows the variation of sensitivity as a function of depth after opposing views are added. The variation in sensitivity still present is not insignificant, particularly in view of the fact that the anterior-posterior dimension of the head is 19 cm compared with 14 cm for the ear-to-ear distance. Since this is the most serious effect which will introduce an undesirable distortion into the resulting image, efforts are now underway to include the effect of attenuation in the calculations.

The influence of the statistical variation in the number of counts collected from each matrix element was studied empirically by varying the total number of counts collected in a set of eight views and observing the influence on the calculated section views.

Regarding the resolution of the camera and its influence on this process, the following can be said. If the resolution of the camera were independent of depth then each of the eight views would image a point source as an approximately Gaussian-shaped spot of the same size. This would be equivalent to observing a similarly shaped source with an ideal camera of infinite resolution as far as this process is concerned. The calculated distribution is thus not a reconstruction of the actual distribution but a reconstruction of the actual distribution as degraded by the limited resolution of the camera. Since resolution of the Anger camera varies slowly as a function of depth, it can be considered a second-order effect and therefore its influence on this process should be small.

All of the above-mentioned factors influence the point-source response function. Thus, instead of the ideal star-shaped response shown in Fig. 2, the point-source response function is affected by attenuation, resolution, scattering, septum penetration in the collimator, and statistics; furthermore it varies as a function of position in the object. Nevertheless its basic shape will be that shown in Fig. 2 but with the edge of the star pattern being not as well defined because of limited resolution, scattering, and septum penetration and with arms of unequal intensity due to attenuation. The iteration scheme described takes into account only the overriding effect—namely the

TABLE 1. ATTENUATION FOR 140-keV GAMMAS AS FUNCTION OF DEPTH IN WATER FOR OBJECT 14 CM IN DIA AS SEEN FROM ONE SIDE (COLUMN A) AND FROM BOTH SIDES (COLUMN B)

Depth (cm)	Attenuation (%)	
	A	B
0	0	0
2	26	20
4	46	32
6	60	38
8	70	38
10	78	32
12	84	20
14	88	0

star pattern—but does not at the same time attempt resolution enhancement or compensation for the other factors mentioned.

APPARATUS

The scintiphotos are obtained using a Pho/Gamma scintillation camera (Nuclear-Chicago Corp.); they are digitized into a 40×40 matrix using a 1,600 channel two-parameter analyzer (Nuclear-Chicago Corp.). The digitized matrices are transferred onto magnetic tape in a computer-compatible format.

Since the eight scintiphotos must be accurately aligned relative to each other, a special positioning device is necessary. A sturdy rotatable chair with a mark every 45 deg was used for the phantom study. For accurate patient positioning, a special chair was constructed. The whole chair is mounted on a movable carriage which slides in a set of tracks so that the chair can be moved at right angles to the plane of the camera, i.e. along the x-axis of Fig. 1, without losing the alignment. For each view the chair is moved as closely as possible to the camera to obtain maximum resolution. To rotate the patient, the chair is pulled back far enough to permit the shoulders to rotate past the camera head. As its main feature, the chair permits rotation of the patient's head relative to the shoulders around an axis which coincides with the axis around which the chair as a whole rotates. This allows rotation of the head by 45 deg and rotation of the chair by 45 deg to allow a lateral view to be taken with only a small space between the patient and the camera. To avoid an excessive feeling of anxiety on the part of the patient, the head is not immobilized completely. Instead, a chin rest is provided as well as a support at the back of the neck which reduces the degrees of freedom substantially but still allows tilting of the head. After each rotation through 45 deg the proper position is re-established by aligning a mark on the patient's head with a plumb suspended from overhead. The basic features of this chair regarding patient positioning can also be incorporated in a specially constructed table, so that the approach can be extended to very sick or uncooperative patients.

COMPUTER PROGRAM

The section views are calculated on an IBM 360/30 computer. Eight digitized scintiphotos are read from the magnetic tape and the proper data points are selected from each. The circular field of view of the scintillation camera, which is somewhat less than 10 in. in diameter, has the form of an inscribed circle in the 40×40 matrix of the multi-

channel analyzer. Thus, each row of data from the matrix corresponds to a slice in the object approximately $\frac{1}{4}$ in. in thickness. Up to 40 section views can therefore be calculated theoretically. Such a large number of section views is neither necessary nor desirable without an adequate display device. Therefore, a variable number of adjacent rows are added—usually three to give a section view of $\frac{3}{4}$ -in. thickness—and a total of approximately six section views are calculated per patient. Adding of adjacent rows also has the advantage of improving the statistics for each section view. Data from opposing views are added in the appropriate fashion, further improving the statistics. Every data point which is less than 3% of the maximum value of all data points is considered to be background and is set equal to zero. From this, the maximum extent of the object can be determined as discussed above. The section view is calculated; the resulting 40×40 numerical matrix is printed out on the line-printer for reference purposes and is also written onto a second magnetic tape. The section views on this output tape can be played back into the multichannel analyzer and viewed on a CRT display in pictorial form. While viewing the CRT display, one can vary background and contrast to enhance different features of the section view. The section views can be calculated with varying amounts of contrast, which largely determines the time to perform these calculations. The average iterative computation consisting of 35 iterations takes 30 sec; the total time per section view is approximately 45 sec. It requires 15 sec to back up the input tape eight views if necessary, read in eight views, check for valid data, find the outline, format the data in a convenient form, print out the section view on the line printer, and write it onto the output tape. The program is written in the Fortran language for the most part; reading from and writing onto magnetic tape as well as the actual iterative calculation is performed using the "Basic Assembly Language" (BAL), which is more flexible for input and output operations and appreciably faster in highly repetitive operations than Fortran.

PHANTOM STUDY

Before applying this process to patients, a phantom study was undertaken. A head phantom was filled with a resin impregnated with a total of 46 μCi of ^{57}Co , of which 40 μCi were spread uniformly throughout the phantom, 5 μCi were concentrated in a circular container 1 in. in diameter and 1.75 in. long near the medulla, and 1 μCi was concentrated in a similar container in the right cerebral hemisphere. The resulting target-to-nontarget ratio was 25:1 and 5:1 respectively. The phantom was placed

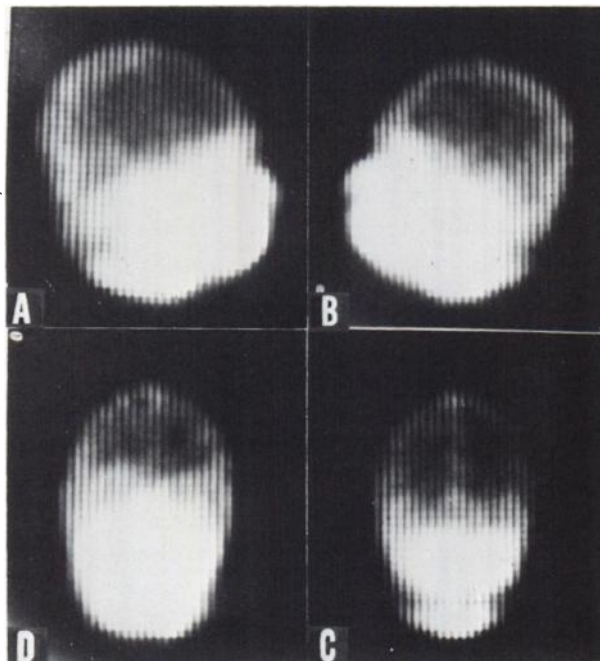


FIG. 5. Four of eight views used to calculate section views, A and B showing right and left lateral respectively, C and D showing posterior and anterior, respectively.

on a rotatable chair and several sets of eight scintiphotos were taken 45 deg apart, varying the total number of counts for the different sets.

Two conclusions drawn from the calculated section views are of importance: (A) the variation of sensitivity due to absorption within the phantom did not cause a noticeable problem; (B) even when the whole set of eight views contained only 150,000 counts (clearly less than would be encountered in a clinical situation) the weak concentration (5:1 target-to-nontarget ratio) was still imaged quite clearly when a section view of $\frac{1}{2}$ in. was calculated. Thus the program performs well in spite of severe statistical fluctuations in the number of counts per channel in the input data.

PATIENT STUDIES

Ten patient studies have been performed to date. Eight views are taken using the chair described above anywhere from 1 to 5 hr after injection of several millicuries of ^{99m}Tc -pertechnetate. Data are accumulated for a constant period of time for all eight views ranging from 40 sec to 2 min, depending upon the counting rate and tolerance of the patient. Generally, each view contains approximately 200,000 counts. A complete study requires approximately 20 min. Six section views were generally calculated per patient, each $\frac{3}{4}$ in. thick. A typical example is shown in Fig. 6C; it was calculated at a level passing just below the eyes. Particularly noteworthy are

the smooth outlines as well as the high contrast. From the digital printout, numerical values for the contrast are easily determined, the ratio of the density in the region of the frontal sinus to the density in the cerebellum is 9:1; the ratio of the density in the peripheral region to that in the cerebellum is 4:1. Thus, regions of low uptake surrounded by regions of higher uptake on all sides are imaged quite well.

Figure 5 shows the four standard scintiphotos, which are part of the input data, as seen on the CRT of the multichannel analyzer for one of the patients; Fig. 6 shows the calculated section views.

In the patient studies performed to date structures were visible in some of the section views which could have been due to either artifacts or actual variations in the isotope concentration. Due to this uncertainty the section images have so far been used only to aid in the localization of concentrations visible in the normal views used to calculate the section views. As the confidence in the section views is increased by clinical experience, it is hoped that the section views can be used to aid in detection as well as in localization.

COMPARISON TO OTHER METHODS

Section imaging is not new in the field of nuclear medicine. Kuhl and his associates have made valuable contributions in longitudinal as well as transverse section scanning over a number of years using a variety of special devices (1). Anger has built a scanning scintillation camera with which longitudinal section views of remarkable resolution have been obtained (7). A number of authors have recently reported on a variety of devices, all in the experimental stage, which are modifications and combinations of the devices mentioned above (8-10). A scheme involving a rotating chair, scintillation camera and a rotating photographic film was also reported by Anger some years ago (3).

In longitudinal section imaging one or several images are obtained in which a given plane in the object is in focus while all other planes are out of focus. This approach has been very successful in radiology and recently also in radioisotope imaging. At least from a conceptual point of view, it seems desirable to eliminate completely information from other planes rather than merely to defocus it. One can certainly imagine situations in which a large volume of overlying activity—even though out of focus—can mask a region of decreased activity above or below it. Whether such situations occur frequently enough to merit serious consideration is a question which undoubtedly will be answered some time in the future. In transverse-section imaging the object

is viewed from different positions around it. The resulting images represent views of the object at right angles to the plane in which the detector moves, and they are obtained by a process of superposition of information from different directions. This makes it difficult to reproduce areas of low activity which are surrounded by areas of higher activity because of the star-like pattern or, in devices using continuous rotation, of the large bell-shaped spot.

The most important difference, however, between the process described here and other schemes is the fact that it is not a separate procedure following a regular brain study using a special device. Instead, an unmodified scintillation camera is used together with equipment already available in a number of hospitals; the chair used for patient positioning is simple and inexpensive. Instead of the four standard views (anterior, posterior, and both laterals), eight views are taken requiring little additional time. After viewing the standard views, the decision can be made to calculate any number of section views at any level with thicknesses variable in $\frac{1}{4}$ -in. increments.

FUTURE DEVELOPMENT

The success achieved in calculating section views of the brain warrants a serious effort to try to expand this process to include other organs, particularly the liver. It should be stressed that so far, it has not been shown, either by us or by anyone else, that the added knowledge gained by knowing the distribution of the radioisotope in three dimensions instead of observing a two-dimensional projection is worth the effort from a medical point of view. The first objective is to obtain a realistic representation of the three-dimensional distribution. This should be most valuable in the case of the liver, which has an irregular shape which varies from person to person and where the problem of overlying activity masking an area of decreased uptake is particularly serious. Unfortunately, this process cannot be applied to liver imaging in a straightforward manner. Particularly bothersome is the problem of radiation attenuation in surrounding tissue since the liver is surrounded by a layer which is not uniformly thick on all sides and which varies considerably from per-

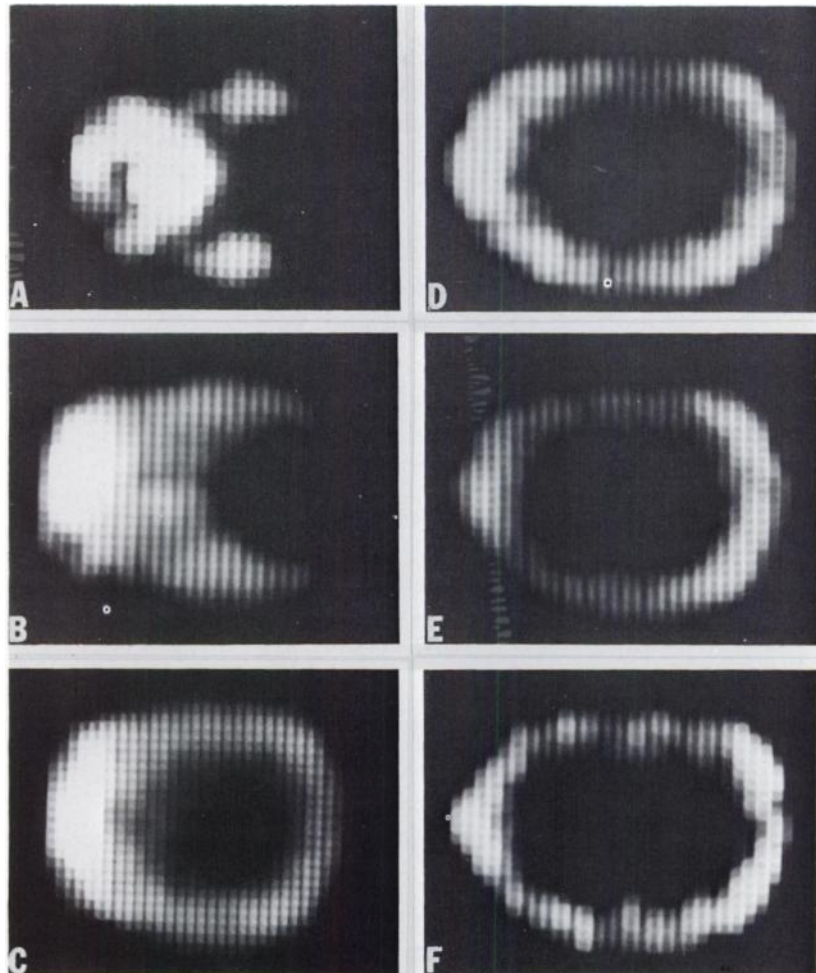


FIG. 6. Section views calculated for same patient. Section views are spaced $\frac{1}{4}$ in. apart; section view A passes through parotid glands. Anterior is towards left.

son to person. Modifying the computer program to compensate for attenuation may well lengthen the time to calculate a section view appreciably. The problem of activity in the spleen which will be present in some views but not in others as well as problem of patient positioning will have to be considered.

SUMMARY AND CONCLUSION

A method has been developed by which section views of the brain are obtained. From a set of eight digitized scintiphotos, which includes the standard anterior, posterior, and lateral views, section views are calculated on an IBM 360/30 computer in a plane at right angles to the scintiphotos. The method has been evaluated clinically and was found to give a good representation of the actual distribution.

Equipment to perform this procedure is becoming available in a growing number of hospitals; access to a large computer is required. Patient positioning is achieved using a modified rotatable chair. The technique requires at the moment, a patient who can cooperate at least minimally, and who is able to sustain the sitting position. As part of a routine brain scan study, the data may be obtained with only a few minutes of extra time on the gamma camera. Although six to eight section views cover the regions of interest within the confines of the cranial cavity, in fact 20–40 section views may be calculated. The section views show high contrast and clearly display the low-level concentration characteristic of normal cerebral tissue compared to surrounding structures in which higher levels of activity produce a greater concentration.

REFERENCES

1. KUHLE DE, EDWARDS RQ: Reorganizing data from transverse section scans of the brain using digital processing. *Radiology* 91: 975–983, 1968 and references contained therein.
2. HARPER PV: The three-dimensional reconstruction of isotope distributions. In *Fundamental Problems in Scanning*, Gottschalk A, Beck RN, eds., Springfield, Charles C. Thomas, 1968, p. 191
3. ANGER HO: Transverse-section tomography with the scintillation camera. *J Nucl Med* 8: 314–315, 1967
4. IINUMA TA, NAGAI T: Image restoration in radioisotope imaging systems. *Phys Med Biol* 12: 501–509, 1967
5. TAUXE WN: Digitization and data processing of scintiscan matrices by high-speed computer. In *Medical Radioisotope Scintigraphy* vol. 1, Vienna, International Atomic Energy Agency, 1969, p. 803
6. WILENSKY S, ASHARE AB, PIZER SM, et al: Computer processing and display of positron scintigrams and dynamic function curves. In *Medical Radioisotope Scintigraphy* vol. 1, Vienna, International Atomic Energy Agency, 1969, p. 815
7. ANGER HO: Tomographic gamma-ray scanner with simultaneous readout of several planes. In *Fundamental Problems in Scanning*, Gottschalk A, Beck RN, eds., Springfield, Charles C. Thomas, 1968, p. 195
8. CASSEN B: Image formation by electronic cross-time correlation of signals from angular ranges of unfocused collimating channels. In *Medical Radioisotope Scintigraphy* vol. 1, Vienna, International Atomic Energy Agency, 1969, p. 107
9. MIRALDI F, DICHIRO G, SKOFF G: Evaluation of current methods of radioisotope tomography and design of a new device: the tomoscanner. *J Nucl Med* 10: 359, 1969
10. PATTON J, BRILL AB, ERICKSON J, et al: A new approach to mapping three-dimensional radionuclide distributions. *J Nucl Med* 10: 363, 1969